CHAPTER 1

PRECISION LUMINOSITY MEASUREMENT

The accelerator machine detector interface (MDI) region has a racetrack beam-pipe optimized for closing up to interaction point and less electromagnetic heating by higer-order-modes of beam propagation with a 33 mRad beam crossing angle at the Interaction Point (IP). The luminometer is instrumented for detecting Bhabha elastic scattering of e^+e^- collisions in the forward region with the Luminosity Calorimeter (LumiCal) implemented in low θ angle region with optimized upstream beam-pipe material and precision detector configuration.

The CEPC is designed with instant luminosity of $8.3 \times 10^{34}/cm^2s$ and $1.9 \times 10^{36}/cm^2s$ at the HZ and Z-pole operation modes (50MW plan), at center of mass energies of $\sqrt{s} = 240$ GeV and 91 GeV, respectively. The expected yield with two IPs are 4 million HZ and 4 trillian Z boson events. With such a high event statistics, the precision on measuring Standard Model processes require a precision on luminosity of better than 10^{-4} at Z-pole.

The cross section of Bhabha interaction is calculated to next-to-leading order correction for the process of $e^+e^- \to e^+e^-\gamma$. The BHLUMI event generator [1] developed at LEP for small angle Bhabha cross section has being improved to 0.037% systematic precision [2]. A recent developed event generator call ReneSANCe [3] has reported consistency with BHLUMI and potential acceptance deviation at the 0.1% level due to radiative Bhabha events with electrons scattered with high θ angles. The high order corrections to Bhabha interaction are being motivated for future e^+e^- collider projects toward 0.01% precision.

At CEPC, Bhabha events are characterized with a pair of electron and position back-to-back in direction, each with momentum of beam energy. The LumiCal consists of two sets of calorimeters surrounding the beam-pipe on on each sides of the IP. Illustrated in Fig. 1.1 are the LumiCal sections in the MDI region. before the beam-pipe flanges on each z-sides are two layers of Si-wafers in front of 2 X_0 scintillation crystals, for detecting electron

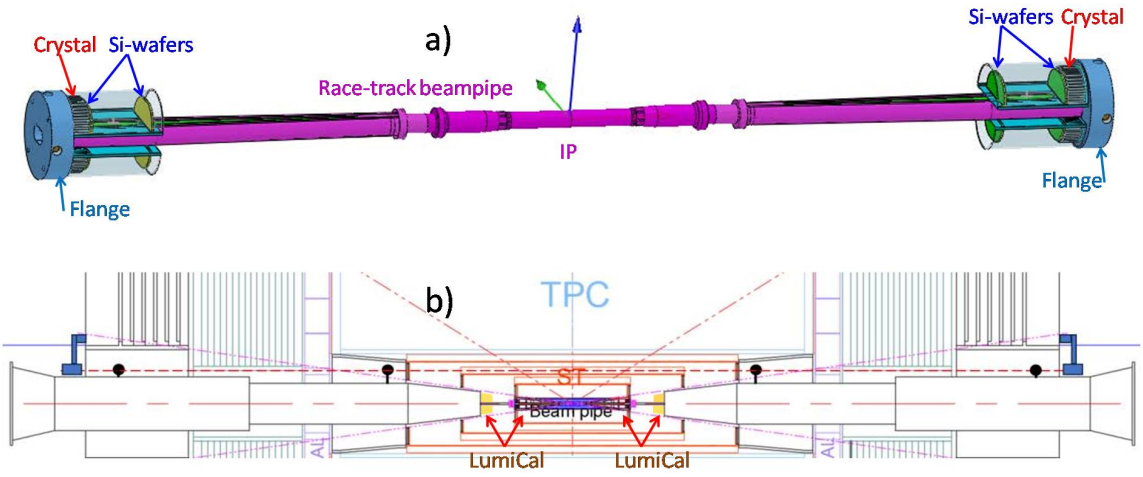

Figure 1.1 The LumiCal in the MDI region is illustrated with the beam-pipe and detectors in a) within the flanges; and b) with crystals in front of the quadruple magnets in yz-view along the beam-pipe.

impact positions and for $e^{\pm}/\gamma$ identification. Behind the flanges and bellows are 20 X_0 of crystals mounted in front of the quadrupole magnets.

At the leading order of Bhabha interaction, the cross section integrated over an angular coverage of ($\theta_{min} < \theta < \theta_{max}$) is,

$$\sigma = \frac{16\pi\alpha^2}{s}\left(\frac{1}{\theta^2_{min}} - \frac{1}{\theta^2_{max}}\right). \tag{1.1}$$

The integrated luminosity ($\mathcal{L}$) with N_{acc} detected is,

$$\mathcal{L} = \frac{1}{\epsilon}\frac{N_{acc}}{\sigma}, \quad \frac{\Delta\mathcal{L}}{\mathcal{L}} \sim \frac{2\Delta\theta}{\theta_{min}}. \tag{1.2}$$

where ϵ is the detection efficiency to be evaluated. The systematic uncertainties are attributed mostly by the error on θ_{min}, mainly due to mechanical alignment and the detector resolution. The error propagates to the luminosity is twice higher.

Assuming that the θ_{min} acceptance for detecting Bhabha can be set to 20 mRad, the corresponding deviation $\Delta\theta$ caussing 10^{-4} error in luminosity is 1 μRad. At a distance of $|z| = 1$ m from the IP, the tolerance is 1μm. The precision on measuring fiducial edges for Bhabha detection is approaching the instrumentation limit.

The location of luminometer is favorable for lower θ_{min} to increase Bhabha cross section with a $1/\theta^2$ dependence. The LumiCal front Si-wafer is located at $|s| = 560$ mm. The race-track beam pipe has an inner radius of 10 mm. Assuming the detector acceptance edge is 12 mm from the beam pipe center, the corresponding θ_{min} is 21.4 mRad. Illustrated in Fig. 1.2.a is the drawing of the beam pipe volume before the flange, and Fig. 1.2.b the LumiCal including the LYSO crystal sector in front of the quadrupole magnet located between $|z| = 900$ to 1100 mm.

The x-y projected LumiCal is plotted in Fig. 1.3.a, with the trace-track beam-pipe expanding from the IP ring of 10 mm diameter to 3 mm thick dual copper pipes. The LumiCal components are separated in modules above and below the beam pipe, the dimension of components before the flange are illustrated in b) for the second layer of Si-wafer and the 2 X_0 LYSO bars.

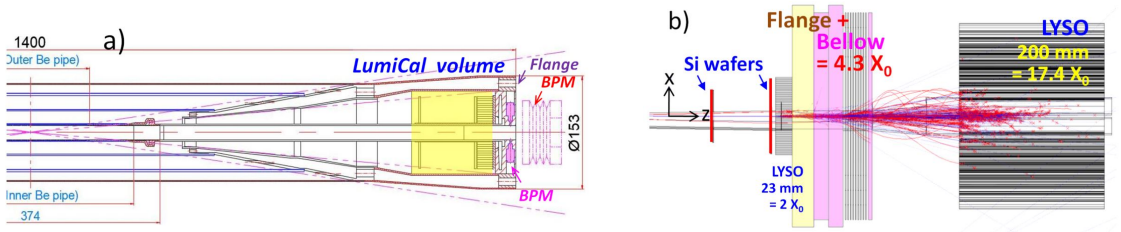

Figure 1.2 The LumiCal volume before the flange is shown in a), where two Si-wafers are positioned before 2 X_0 LYSO bars. Inside the flanges in each side, four Beam Position Monitors are installed. b) the LumiCal is shown with a 50 GeV electron shower illustrated. Before the flange, the Si-wafers with short LYSO crystals provide electron θ position with e/γ veto. The long LYSO behind the bellow provide beam electron identification by energy deposits.

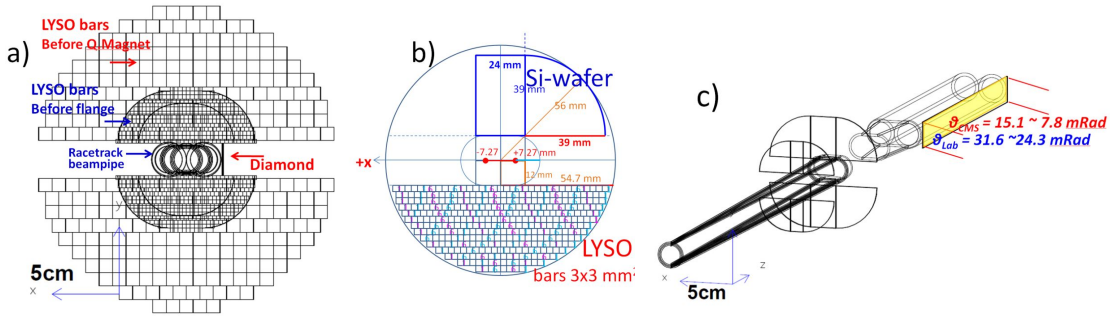

Figure 1.3 The projection of LumiCal design is illustrated in a), with the racetrack beam pipe from IP to quadrupole. The design of the second Si-wafer at $|z| = 640$ mm and the 2 X_0 of LYSO bars mounted on the flanges are plotted in b). The front LYSO bars dimension is $3 \times 3 \times 23$ mm^3. The 17.4 X_0 LYSO modules in front of quadrupole magnet are segmented in $10 \times 10 \times 200$ mm^3. The fast monitoring diamond detectors in c) are positioned between the long LYSO modules on the sides of electron boosted direction, where the Bhabha electron rate is the highest.

The fast luminosity monitor is planned for beam-stealing with Bhabha events at the lowest θ region, on the sides of beam-pipe of the beam boosting direction, between the long LYSO modules. This corner has the highest event rates within the whole CEPC detector volume with scattered Bhabha electrons well described by the QED theory.

In Section 1.1 we first discuss the fast luminosity monitor, for beam steering on the counting rate of Bhabha electrons, and as a on-line Luminomiter. The detector option is discussed for a fine pitch diamond strip detector that can endure the strong radiation field. The prototyping with strip implantation and the response to MIP traversing are discussed.

The Bhabha acceptance in the MDI volume is investigate with the BHLUMI which is discussed in Section 1.2, for the LumiCal coverage corresponding to $r = 25$ mRad, $|y| > 25$ mm at $|z| = 1000$ mm. With both scattered electrons of Bhabha events detected, the cross section (78 nb) at Z-pole is about twice of the $Z \to q\bar{q}$ channel (41 nb) for Z line-shape study.

The BHLUMI generator is developed and employed at LEP for Bhabha events based on the YSF exponetiation algorithm, and the latest refined version reached 0.03 % systematic uncertainty. Bhabha calculation on Feynman diagrams are approaching 0.01 % precision. Measurement of radiative Bhabha with initial or final state radiations shall be conducted to confirm the theoredical NLO description. In Section 1.3 the radiative photons of BHLUMI

and the ReneSANCe programs are compared and the measurement with e, γ of radiative Bhabha are estimated.

The LumiCal design has evolved with the beam pipe design, from the original 30 mm round pipe, to the laste race-track design. The ealiest detector technology has assumed a Si-W sandwiched assembly, reported in CDR. To accommodate the limited space in the forward MDI region, the latest assembly with Si-Wafers and LYSO crystals is discussed in Section 1.4.

The systematic errors occur on the edge of fiducial acceptance for Bhabha event counting. The 10^{-4} precision corresponds to 1 mRad at $\theta = 20$ mRad. During the detector accembly, the Si-wafer edges can be located by industrial survey equipments to sub-micron precision. However, once installed on the MDI, the position monitoring shall be instrumented. The electron beam position is monitored by several sets of Beam Position monitors inserted inside the MDI flanges, and before quadrupole magnets. The position offsets of MDI components shall be considered for vibrations and thermal expansion, etc, can be significant. The survey precision derived to luminosity measurement error is discussed in Section 1.7.

1.1 Fast Luminosity Monitor

The fast luminosity monitor is consider for instant feedback of beam collisions for steering of beam position with external detectors. We propose for detecting scattering of small angle Bhabha electrons in the detector volume. The location is by the beam pipe before the quadrupole magnet, where the polar angle corresponds to $\theta \sim 10$ mRad. This corner has the highest e^+e^- collisions events, in part due to the beam-cross of 33 mRad to boost small angle Bhabha electrons out of beam pipe.

Illustrated in Fig. 1.4.a is a shower event of a 50 GeV electron traversing the 3 mm copper beam pipe at 10 mRad. In Fig. 1.4.b the Bhabha electrons of BHLUMI are plotted surrounding the beam-pipe between $|z| = 900$ to 1110 mm, where the LYSO crystals are located before the quadrupole magnet. The blue bar indicate the location of fast luminosity monitor. At this position, the radiation field is the highest at CEPC. The most radiation

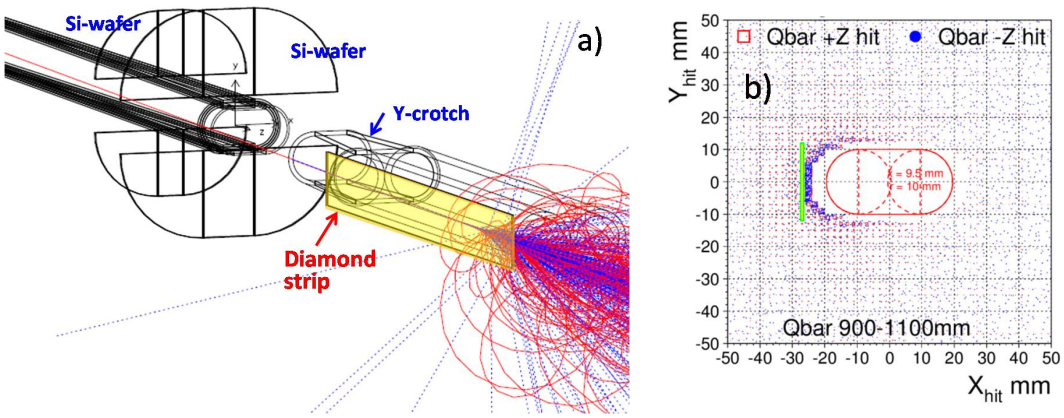

Figure 1.4 a) an event display of GEANT simulation for a 50 GeV electron at 10 mRad to the outgoing beam line, traversing 3 mm thick copper beam pipe; b) x-y distribution of electrons entering LYSO between $|z| = 900$ to 1100 mm.

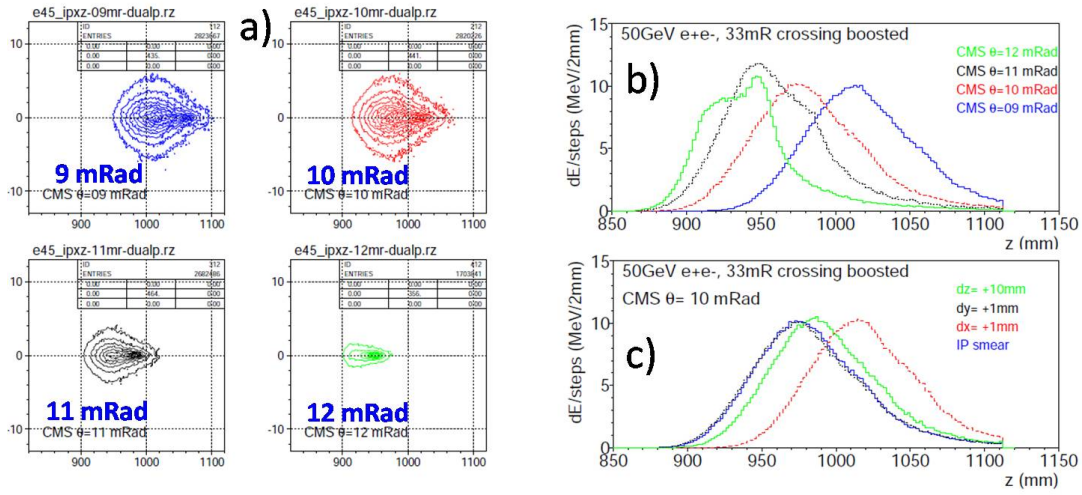

Figure 1.5 Eletron shower profiles are shown a) the y-z counters with CMS θ from 9 to 12 mRad, being boosted ($+16.5$ mRad), at $y = 0$/ The dE/dx deposition in z is shown in b). The sensitivity to IP offsets are plotted in c).

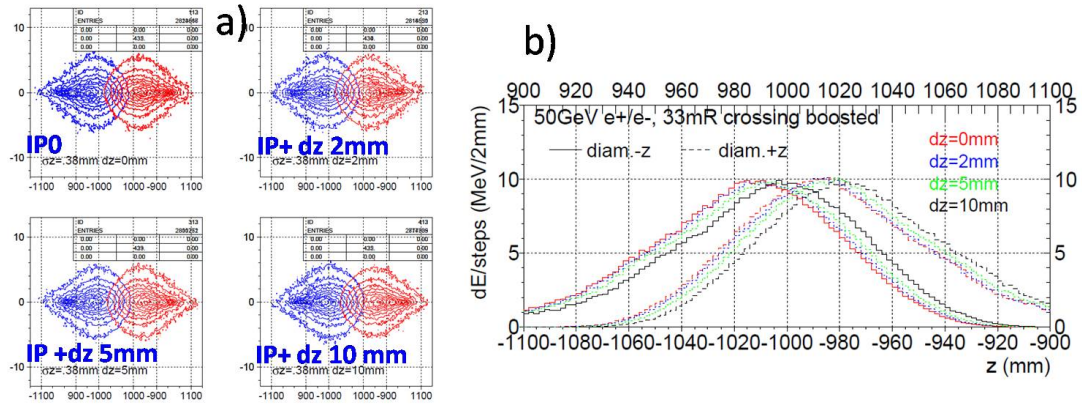

Figure 1.6 a) the contours of y-z shower profiles of both z-sides are shown for various dz offsets of IP; the corresponding dE/dx profiles in z plotted in b).

tolerant detector to be considered is a diamond slab segmented in strips to detect electron showers generated in the copper beam pipe.

The eletron shower profiles generated in the 3 mm copper beam pipe is investigated with GEANT, with tubes positioned parallel to z-axis at center $|x| = 13mm$ and 0.4 mm thick diamond slab at $x = -27$ mm, with the height of $y = \pm 12$ and length $|z| = 855$ to 1110 mm. Electrons were generated at around 10 mRad at $y = 0$ to the diamond. The beam-crossing of 33 mRad corresponds to boost of 16.5 mRad to the electrons. Fig. 1.5.a show the y-z contours of 50 GeV electron showers are theta angles from 9 to 12 mRad, showing a offsets of wide distributions with RMS of 30 mm (Fig. 1.5.b). The shower profiles are compared for offsets of the IP, that may help beam steering. The deviation on x position can be sensitive to 0.1 mm level, and z position deviation of around 10 mm.

The fast luminosity monitors assist beam steering by observing scattering of electrons on both z-sides. The electrons shower profiles are observed event by event. The integrated events rates along the z-positions can help monitoring the z-position of IP. Illustrated in

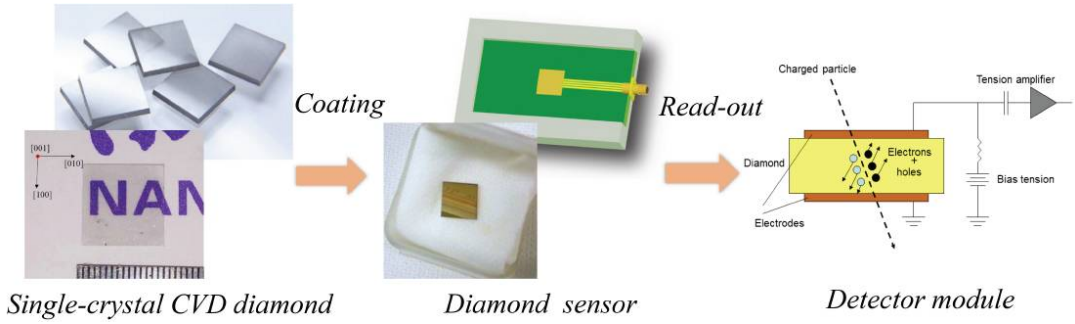

Figure 1.7 Fabrication process of CVD diamond detector module.

Fig. 1.6.a are the contours of both z-sides with dz offsets of IP. The corresponding dE/dx beam profiles are plotted in Fig. 1.6.b.

The diamond detector has the most profound radiation hardness, that can be instrumented as strip detectors. Illustrated in Fig. 1.7 are examples instrumenting diamond detectors. We have started practice implementation of 1 mm pitch strips on a 10×10 sample diamond wafers. The uniformity of strips and signals will be examined to provide options on assembly of a large area slab of around 20×300 mm^2 large diamond monitors.

The beam steering devices around the IP include the BPMs positioned inside flanges on both z-sides, and on dual pipes before the quadrupole magnets. Illustrated in Fig. 1.8.a is the beam-pipe locations of button-type BPMs. In Fig. 1.8.b to d are the BES II measurement of BPM pulses with single positron beam in 4-pole and dual beams in 8-pole BPMs. The pulse heights correlates the beam positions, which are calibrated to measure the true x-y position of the beam currents.

In Fig. 1.9 the BPM field and the iteration for the true beam posiiton is shown. The resolution at CEPC is designed for 1 μm, and the accuracy is estimated for ~ 50 μm.

The IP position at CEPC can be measured with the BPMs, by improving survey of the BPM positions, and by steering the beam with timing precision. The BPMs in the flange

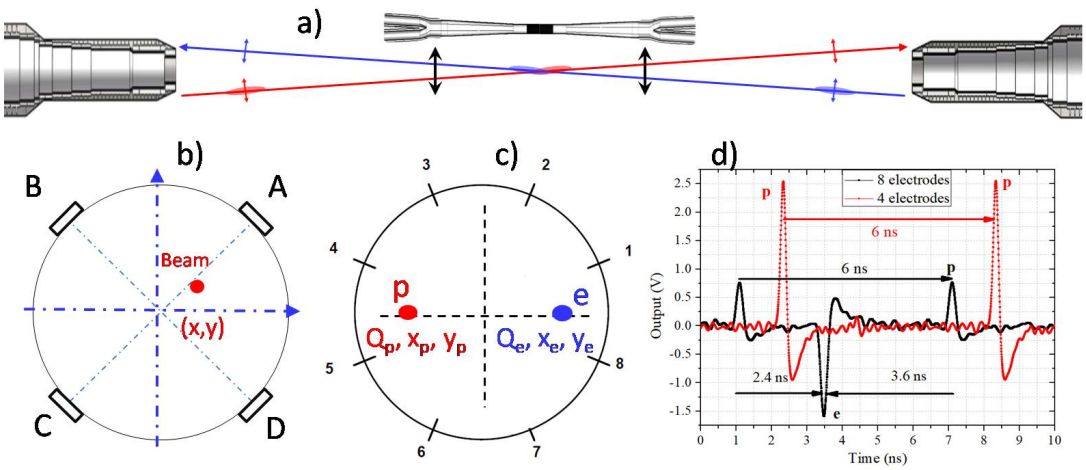

Figure 1.8 The beam position monitors (BPMs) inside flanges will have detect beam bunches that can steer the IP z position. The BPMs single beam pipes before the quadrupole magnets can be precise to 1 μm on the beam x,y positions.

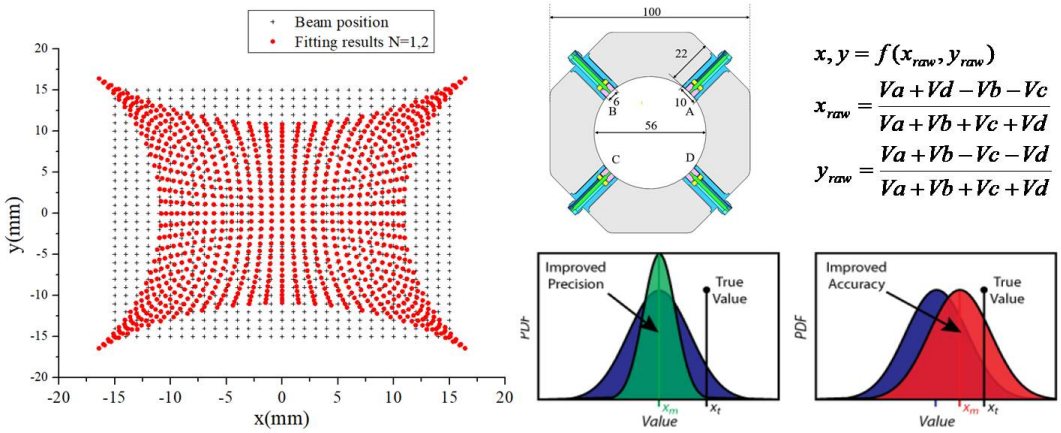

Figure 1.9 The beam position monitors (BPMs) inside flanges will have detect beam bunches that can steer the IP z position. The BPMs single beam pipes before the quadrupole magnets can be precise to 1 μm on the beam x,y positions.

can be measured with fine-tune to ideal positions, so as to minimize distortion of the field map.

The x-y positions of each BPM set can have rather precise resolution of 1μm, the accuracy requires external references may not be easily calibrated

1.2 LumiCal acceptance

The LumiCal detector acceptance is optimized for elastic scattering of Bhabha events, with electrons boosted toward outgoing beam pipe direction. A lower θ fiducial angle to the beam center yield larger acceptance. The distribution of scattered electrons is simulated with the BHLUMI. Illustrated in Fig. 1.10.a are the θ distributions of scattered electrons at CMS frame and being boosted for the 33 mRad beam crossing in Lab frame. The back-to-back angles are also plotted in Fig. 1.10.b.

The event selection for the BHLUMI generated Bhabha electrons has applied parameters previously employed in LEP applications. The Acc0 requires $10 < \theta 80$ mRad in CMS frame, and the Acc1 for $s'/s > 0.5$ with s' the invariant mass of scattered e^+, e^-. The boosted distributions in Fig. 1.10 are selected for the detector acceptance with $r > 25$ mm to the beam centers at $|z| = 1000$ mm, corresponding to $\theta > 25$ mRad, and $|y| > 25mm$ with a flat edges parallel to the race-track beam-pipe surfaces.

In Fig. 1.11 are the distributions of event selections a) with one electron in fiducial region, and b) both electrons in fiducial region. The cross sections are derived for the BHLUMI calculation and the acceptance in fiducial region, which are listed in Table 1.1, the cross sections of generated to the selected, with one or both electrons detected are listed, for the lower θ cuts of 20 and 25 mRad. The slight lower angle has the near twice the cross section. The boost effect push events along the x-axis into the beam-pipe, thus gain is only about 10% asking for both electrons detected. For easier instrumentation, that is reason to cut off band corresponding to $|y| < 25$ mm at $|z| = 1000$ mm.

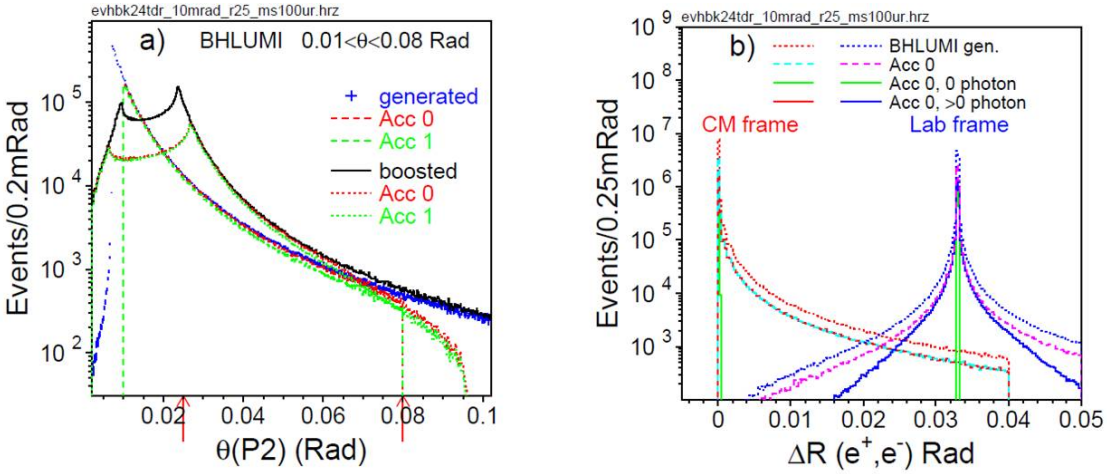

Figure 1.10 a) scattered electron distributions of BHLUMI simulations at CMS frame and after boost for the 33 mRad beam crossing at CEPC. Events are generated for $10 < \theta < 80$ mRad. The Acc0, Acc1 are selections according to the BHLUMI for LEP applications. b) the back-to-back angles of e^+ and e^- are plotted for the generated and boosted, and the Acc0 selected with and without radiative photon.

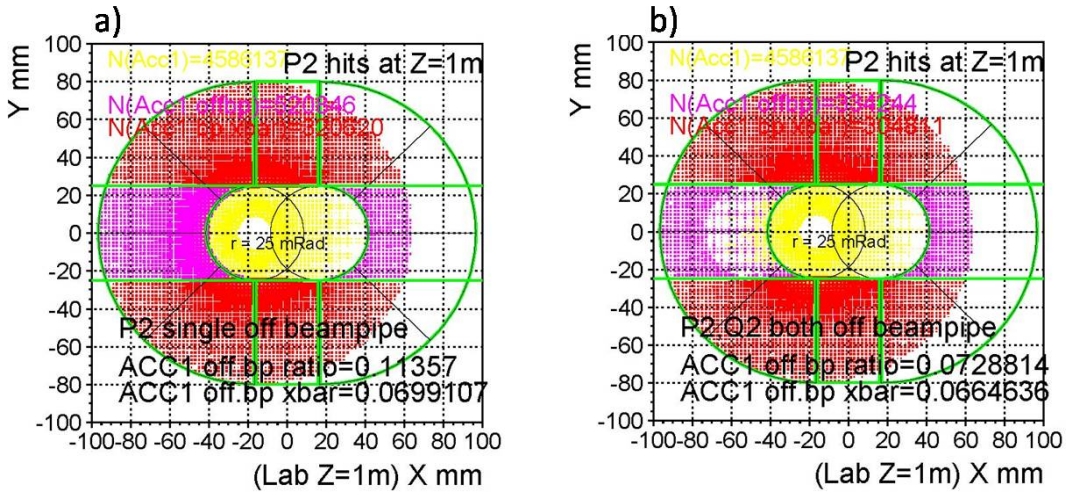

Figure 1.11 a) scattered electron distributions of BHLUMI simulations at CMS frame and after boost for the 33 mRad beam crossing at CEPC. Events are generated for $10 < \theta < 80$ mRad. The Acc0, Acc1 are selections according to the BHLUMI for LEP applications. b) the back-to-back angles of e^+ and e^- are plotted for the generated and boosted, and the Acc0 selected with and without radiative photon.

1.3 Detecting radiative Bhabha events

The BHLUMI generator offers the most precision of 0.037% precision [2] with uncertainties of missing photonic $\mathcal{O}(\alpha^2 L)$ and the hadronic $\Delta\alpha_{had}$ corrections. New calculations with complete NNLO may reach 10^{-1} precision. Radiation Bhabha events cause deviation of electron directions that may smear the event counting crossing the θ_{min} fiducial edge. Therefore measurement of $e^+e^-\gamma$ with ISR and FSR photons are critical to testify the systematic due to radiative Bhabha effect.

Illustrated in Fig. **??** are the comparison of BHLUMI and the newly reported ReneSance program. In a) the Bhabha cross section with $\theta_{min} > 30$ mRad is plotted for the CEPC

	generated	LAB (P2) one electron		LAB (P2,Q2) both electrons	
	BARE1	(mRad)	(mm)	(mRad)	(mm)
		$r > 20$	.and. $\|y\| > 20$	$r > 20$	.and. $\|y\| > 20$
events	457232	84871	53724	54941	51360
σ (nb)	1168.3	216.9	137.3	140.4	131.2
		$r > 25$	.and. $\|y\| > 25$	$r > 25$	.and. $\|y\| > 25$
events	457232	52262	32019	33415	30512
σ (nb)	1168.3	133.5	81.8	85.4	78.0

Table 1.1 Acceptance for Bhabha events simulated with the BHLUMI. The BARE1 is the BHLUMI generated in (Th1,Th2) of (10,80) mRad. The selections are listed for θ to beam centers and y cuts at $|z| = 1000$ mm, corresponding to 20 mRad and 25 mRad to z axis.

center-of-mass energies. The NLO radiation photon momentum are compared in b). The photon energy spectra of both programs agree well.

The photons of BHLUMI are similated with the YFS exponentiation, for the interaction of $e^+e^- \to e^+e^-(n\gamma)$. Photons are not indicated for its radiative source electrons. Illustrated in Fig. 1.13.a are energies of the scattered electron versus the most energetic photon in the same hemisphere. The most energetic photon in a event is analyzed for the opening angles to the electrons, and are identified for the mother electron to be an initial (ISR) or final state radiation photon (FSR), in the LumiCal front LYSO acceptance of $|y| > 12$ mm at $|z| = 647$ mm. In Fig. 1.13.a photon energy versus the opening angle to the closest electron, thus identified as ISR or FSR. ISR photons shall have a large angle to enter the Si-wafer, and the angle to the scattered electron are not correlated by a large angle of > 15 mRad. The FSR photon accompany its mother electron with the opening angle mostly below 5 mRad (91%).

The BHLUMI simulation has 10 M events generated in the θ range of (Th1,Th2) of (10,80) mRad. The e^+ and e^- traveling in each z-direction have 39.7% of them accompanied with radiative one or more photons with energies > 5 5 MeV. The most energetic photon is identified to be an ISR (20.4%) or a FSR (19.4%). In Table 1.2 the events with both scattered e^+ and e^- accepted in front of the LYSO ($|z| = 647$ mm) with $|y| > 12$

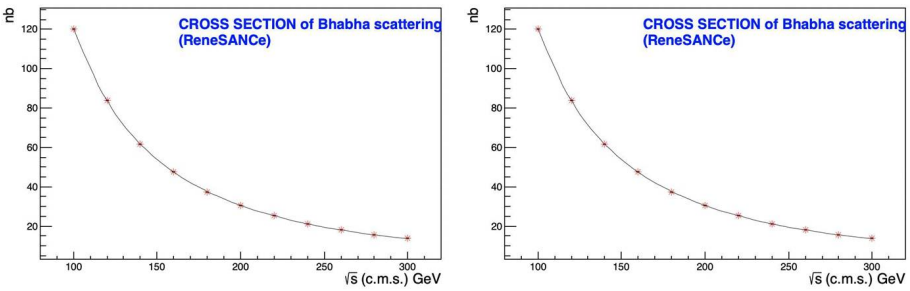

Figure 1.12 Bhabha events are simulated with the BHLUMI and ReneSANce programs which agree well on cross section. In a) the cross sections of ReneSANce is plotted for $\sqrt{s}$ range at CEPC. The radiative photon momenta of both programs are compared and plotted in b).

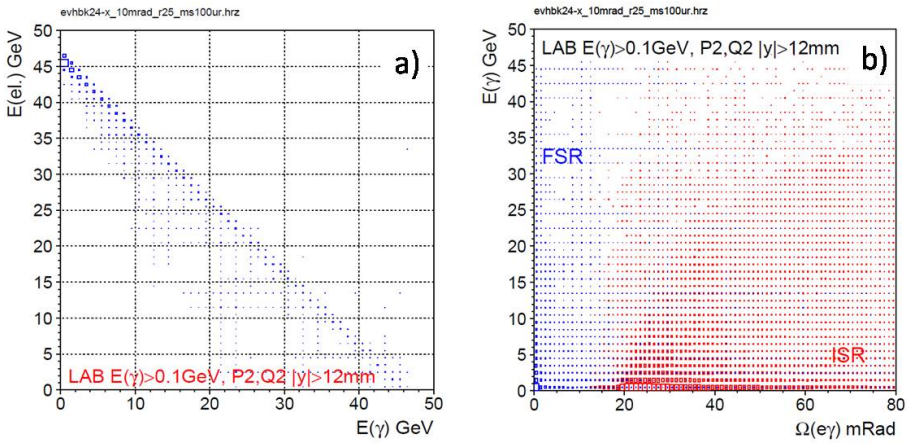

Figure 1.13 The most energetic photon is identified as an ISR or FSR by the opening angle to the closest electron: a) energies of the scattered electron versus the most energetic photon in the same hemisphere; b) photon energy versus opening angle of the most energetic photon to the scattered electron in the same hemisphere.

	$\|y(e^{\pm})\| > 12$ mm		$\|y(e^{\pm})\| > 12$ mm ; $E_\gamma > 0.1$ GeV			$\|y(e^{\pm},\gamma)\| > 12$ mm ; $E_\gamma > 0.1$ GeV			
	$e^{\pm}, 0\gamma, n\gamma$	$e^{\pm}$,γ	$e^{\pm}$,nγ	$e^{\pm}$,ISR	$e^{\pm}$,FSR	$e^{\pm}$,nγ	$e^{\pm}$,ISR	$e^{\pm}$,FSR	$\Omega(e$,FSR) > 5 mRad
events	1405230	631622	445566	233828	211738	206845	12440	194405	41612
ratio	100%	44.9%	31.7%	16.6%	15.1%	14.7%	0.89%	13.8%	2.96%

Table 1.2 The BARE1 is the BHLUMI generated in (Th1,Th2) of (10,80) mRad. The selections are listed for θ to beam centers and y cuts at $|z| = 1000$ mm, corresponding to 20 mRad and 25 mRad to z axis.

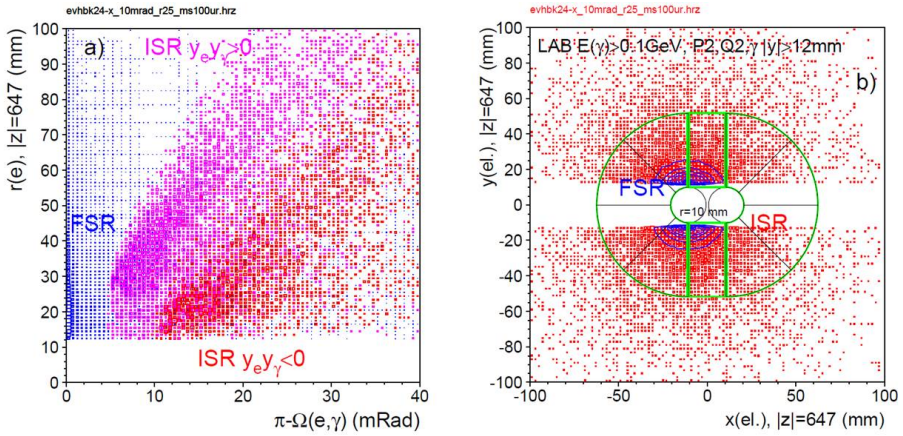

Figure 1.14 Event with radiative photon ($E_\gamma > 0.1$ GeV) are plotted for e, γ separation. a) the scattered electron position in front of LYSO is plotted for the LAB frame x-y radius vs e, γ opening angle in the same z-hemisphere. b) the electron hit positions in LAB x-y frame are shown. In case of FSR both e and γ are close beam pipe; with an ISR, e and γ are spread wider.

mm are counted for the fractions with photon, with > 0.1 GeV photon, wand with photon $|y| > 12$ mm in the LYSO acceptance.

The ISR to be detected in LYSO has a minimal 18.5 mRad (atan(12/647) off the colliding electron, therefore the event fraction is small (0.89%). The scattered electrons closely

accompanied with a FSR is plenty (13.8%). To distinguish the FSR with an opening angle of 5 mRad (8.9% of 0.1 GeV FSR), from the electron, the event fraction is 2.96%.

The e, γ separation is conducted with the hits on Si-wafer and LYSO bar dE/dx deposits. The LYSO segmentation of 3×3 mm^2 corresponds to a pitch of 5 mRad. Plotted in Fig. 1.14.a are the radius of scattered electron in the LAB frame, versus the opening angle to the photon in same z-hemisphere. FSR photons are closely accopanied, and ISRs are in to bands with e, γ in the same y sides or opposite. The electron hit positions with an ISR or FSR are plotted in Fig. 1.14.b. With an ISR the electron hits are scattered more toward larger radius.

1.4 LumiCal detector simulation

The primary goal of the LumiCal is for counting Bhabha events with precision on scattered electron θ in fiducial regions so as to provide an integrated luminosity precision to 10^{-4}. The LumiCal detector options shall be considered for

1. precision of the electron impact position to $r \sim 10$ μm (1 μm) for the errors on luminosity, corresponding to the systematic errors on luminosity of $\Delta L \sim 10^{-3}$ (10^{-4}) in the Higgs (Z-pole) operations;
2. monitoring of the detector alignment and calibration of detector position by tracking of Bhabha electrons with upstream detectors;
3. energy resolution and separation of e/γ for measurements of single photons and radiative Bhabha events.
4. maximum coverage and segmentation of the LumiCal to accommodate the dual beampipe and the beam crossing of 33 mrad;
5. minimizing shower leakage into the central tracking volume.

The LumiCal design has to encorporate the space available in the MDI region, to enlarge the θ coverge. Illustrated in Fig. 1.15 are the drawings of LumiCal modules mounted

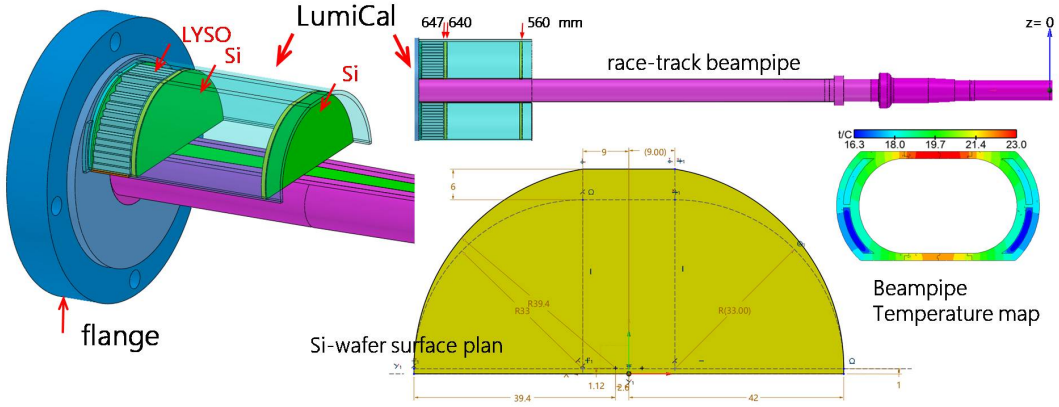

Figure 1.15 Mechanical drawings of the LumiCal modules before the flange of race-track beampipe. The two Si-wafers and $2X_0$ LYSO crystal bars are contained in half circule tubes above and below the pipe. The cooling of beam pipe has the water injected from the flange toward IP within the double Aluminium layers on the sides with the temperature map illustrated.

on the race-track pipe. The Si-wafers measure electron impact position. The best resolution, e.g. with 50 μm pitch strips, can reach 5 μm. The upstream material is the beam-pipe, with double layer of Aluminum containing cooling water circulating from the Flange toward IP.

The Bhabha electrons and radiative photons are generated with the BHLUMI. The detector simulation with GEANT provides multiple scattering and electromagnetic showers in LumiCal. Although the Si-wafer can be instrumented to reach 5μm, the low angle of electrons traversing the thin beam-pipe accumulate a rather thick radiation length. With 1 mm thick Be pipe, the traversing distance at 25 mRad is $(1/\tan\theta)$ is 40 mm, corresponding to $0.114X_0$. With an Al pipe, the corresponding radiation length is $0.45X0$

The beam-pipe near the Si-wafer has Be low-mass windows on the flat section, 6 mm wide, is illustrated in Fig. 1.16.a. The simulation of multiple scattering using 50 GeV muon is illustrated in Fig. 1.16.b before the frange, and Fig. 1.16.c after passing $2X_0$ of LYSO, $4.3X_0$ of steel flange (30 mm) and bellow (45 mm) on to the 200 mm long LYSO bars.

Bhabha electrons are distributed near the outgoing pipe. The smearing due to multiple scattering with BHLUMI generated elestrons are plotted in Fig. 1.17.a for the hits on the

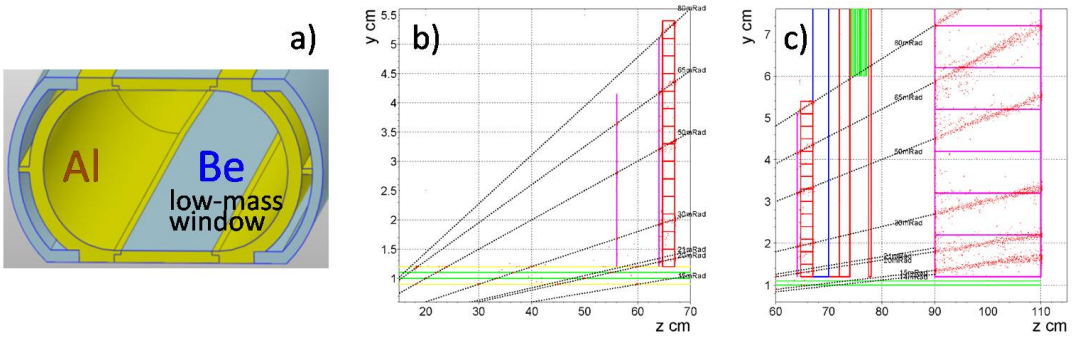

Figure 1.16 a) the beam-pipe has low-mass window with 1 mm thick Be flat layer of 6 mm wide. The multiple scattering is simulated with GEANT The hits of 50 GeV muons are simulated at fixed theta angle traversing Si-wafers and LYSO before flange, and c) passing through flange, bellow to the $17.4X_0$ LYSO.,

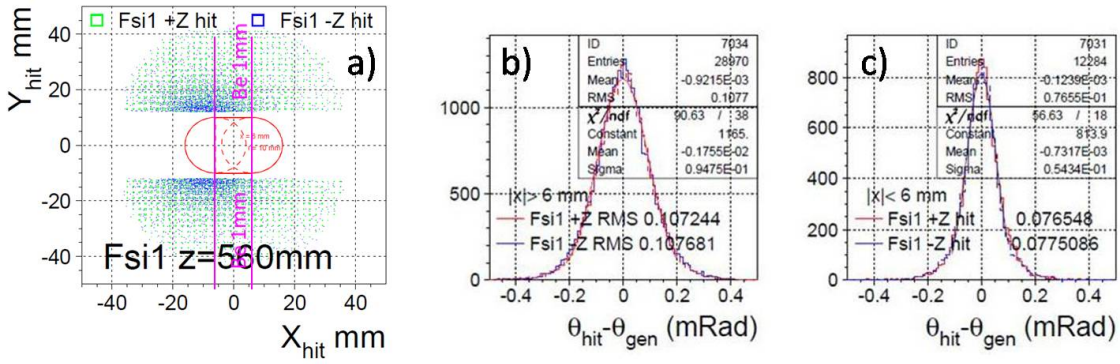

Figure 1.17 BHLUMI generator electrons at $\sqrt{s} = 92.3$ GeV are injected in GEANT LumiCal simulations for multiple scattering effects. a) the hits of electrons on the front Si-wafer at $|zx| = 560$ mm. The beam-pipe has 6 mm wide Be low-mass window as indicated, surrounded by 1 mm Al round pipe. The hits to the generated projection is plotted in b) and c) for $|x|$ outside/within 6 mm, respectively, with Gaussian fits.

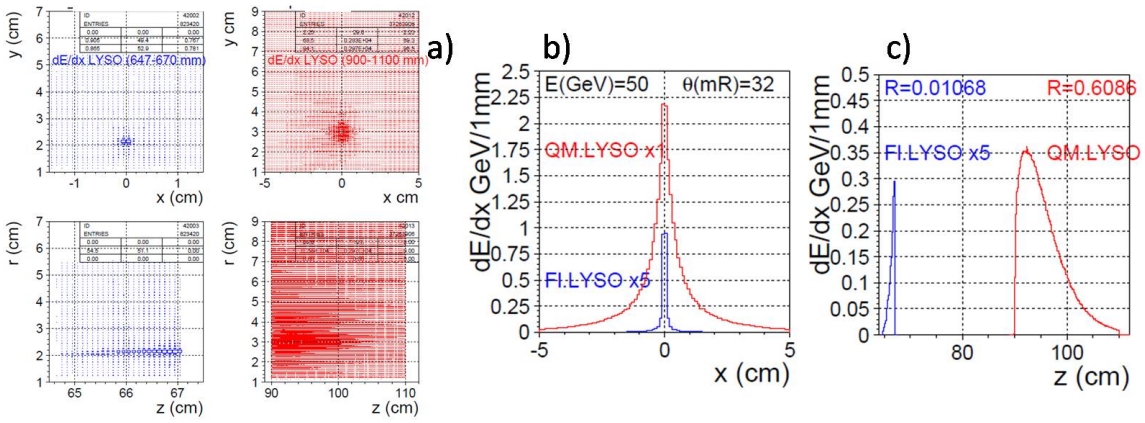

Figure 1.18 Electromagnetic shower of 50 GeV electrons at 32 mRad vertical at 90°. The dE/dx deposits are plotted in the LYSO modules of $2X_0$ before flange (Fl.LYSO) and $17.4X_0$ before the quadruple magnet (QM.LYSO). In a) the dE/dx deposits are plotted in x-y and x-z positions, projection in x axis and z axes.

front Si-wafer at $|z| = 560$ mm, where the 1mm Be window is indicated. The smearing by multiple scattering with all Bhabha electrons, with hit position to the genetated projection, are plotted in b) and c) for the hits outside/inside the $|x| < 6$ mm Be window. The Gaussian fits yield

$$|x| > 6\text{mm}: \quad m = -1.8 \pm 0.6\ \mu\text{Rad} \quad 95 \pm 0.6\ \mu\text{Rad} \tag{1.3}$$

$$|x| < 6\text{mm}: \quad m = -0.7 \pm 0.6\ \mu\text{Rad} \quad 54 \pm 0.7\ \mu\text{Rad}. \tag{1.4}$$

The effects smearing by multiple scattering are symmetric for both the Be low-mass and Al pipes, that is, events being smeared to both sizes are equal. The errors on the mean are less than 1 μRad. At $|z| = 560$ mm, most electrons enter Si-wafer of $|y| > 12$ mm have the $\theta > 21$ mRad, corresponding to $\Delta\theta = 1$ μRad for $\Delta\mathcal{L}/\mathcal{L} = 10^{-4}$ (eq. 1.2).

The simulation in Fig. 1.17 has applied the beam spot size of $\sigma_x = 6$ μm and $\sigma_z = 9$ mm ($\sigma_y = 35$ nm is neglected). The beam-cross results to an overlap of $\sigma_z = 380$ μm in z. If σ_x, σ_z are 0, the Gaussian widths reduce by 5%.

For the accuracy on event counting at fiducial edge, the smearing effect shall be measure so as to measure the mean and error. The two Si-wafer can cross refer each other, to measure the multiple scattering spectra, so as to determine the error on mean for the fiducial edge.

1.5 Shower leakage to tracking volume

1.6 Systematics to 10^{-4} luminosity precision

The detector option for LumiCal is constrainted by the space and weight. The $2X_0$ LYSO crystal covering the radius of 42 mm, 23 mm in length, has a total weight of 0.45 kg ($\pi \times 4.2^2/2 \times 2.3$, density 7.1 g/cm^3, Fig. 1.15). the long LYSO has 10 layers of $10 \times 10 \times 200$ mm^3 bars, corresponding to a total weight of $\pi \times 10^2/2 \times 20 \times 7.1$ of 22.3 kg.

Silicon strip detectors of 50 μm readout pitch is commonly reaching a resolution of $\sigma \sim 5$ μm. The alignment of the detector position would be the major systematic requirement for an absolute precision of better than 1 μm. Single event measurement has much larger error to the required 1μRad precision, however, the mean on error ($\bar{\sigma} = \sigma/\sqrt{n}$) would

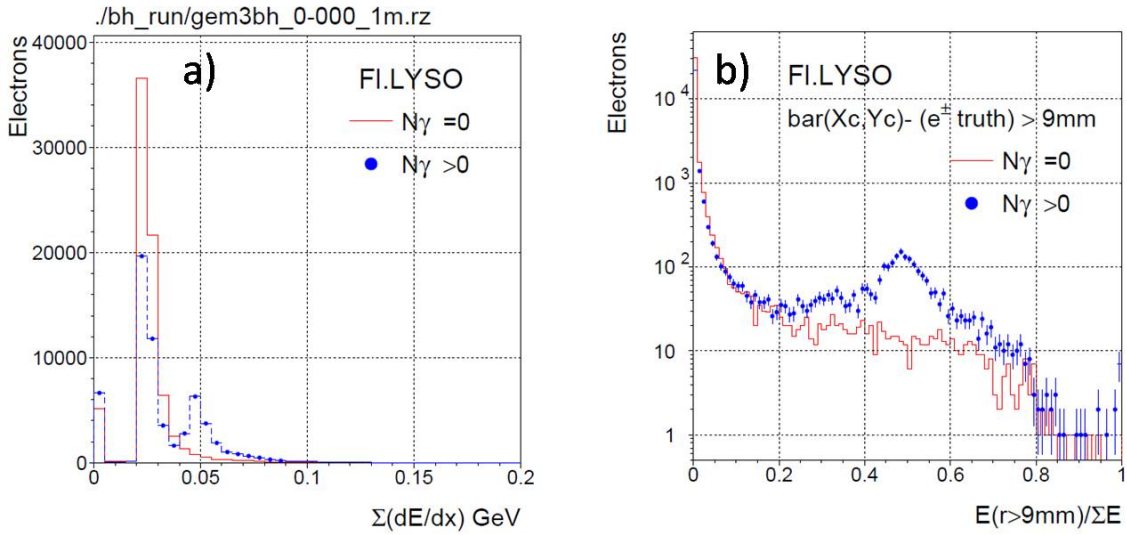

Figure 1.19 Electrom

be much smaller. The issue is for survey and monitoring precision on the fiducial edge for Bhabha event acceptance. The mean of fiducial edge and the systematics to it are the LumiCal design goal.

The segmentation of the calorimeter is considered for the back-to-back resolution detecting a pair of Bhabha electrons, and for separation of e/γ in the presence of radiative photon accompanied with the electron or from beam background. The thickness is determined for the energy resolution favorable of $> 20X_0$ for shower containment of a 50 GeV electron.

The alignment precision of the front-layer Silicon detector is the most critical issue to reach 1 μm in radiaus for the luminosity measurement of 10^{-4}. An online survey system is required to monitor the fiducial edge position.

The theta angle of a detected electron is calculated assuming an IP position measured by the beam steering and the central tracking system. The IP position relative to the luminosity detector could be limited to survey relative to central tracking devices or beam pipe.

The back-to-back tracking of the pair of Bhabha electrons will also provide calibration for detector position. The front silicon layer of the luminosity detector will measure electron impact positions to a few micron. This wafer shall be an 2D fine-pitch strip detector, the position is measured by strips collecting the ionization charges generated by a traversing electron.

The boost is toward $+x$ direction of the laboratory frame. The electron impact positions on the LumiCal front-layer at $z = 100$ cm are also plotted in Fig. 1.20, in slices of every 45 degrees to indicate the dependence on p_T direction. The beam-pipe centers are at $x = \pm 16.5$ mm. The green lines indicate the beam-pipe area of 20 mm in radius extending horizontally, and the coverage of the LumiCal in segmentation of circular and rectangular silicon wafers. The electron impact positions are illustrated for >20 mRad to the laboratory frame. Electrons of low scattering angles, in particular for those in $-x$ direction, are lost into beam-pipe. To have both scattered electrons and positrons detected, the corresponding θ_{min} on the horizontal axis is the beam-pipe acceptance plus

16.5 mRad. The loss of vents on vertical direction is much less. With a beam-pipe as indicated with $\pm y$ dimension equals radius, the horizontal boost is not losing electrons with a larger y-position.

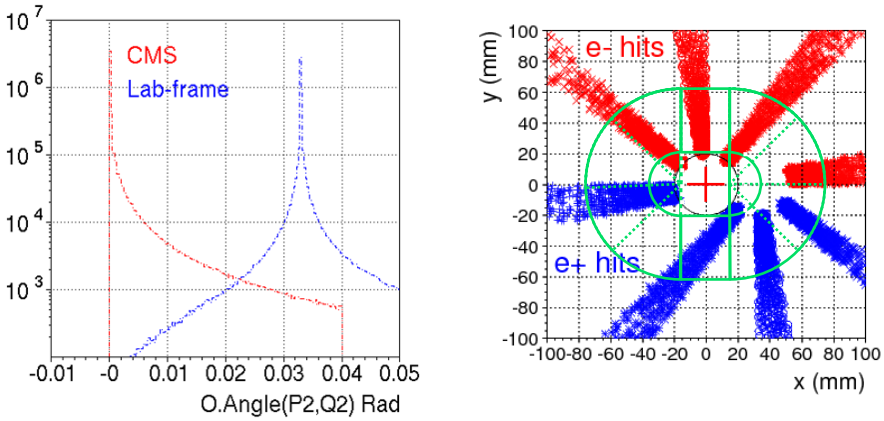

Figure 1.20 Bhabha events of BHLUMI simulation at the Z-pole are plotted for the back-to-back opening angle of scattered electron-position pairs in Center-of-Mass and the laboratory frames (left). The impact positions on the LumiCal front face are plotted in slides of ϕ angles every 45 degrees (right). The detector coverage is illustrated in green lines indicating a beam-pipe of 20 mm, extended from beam center at $x = \pm 16.5$ mm.

The TUBE configuration leaves a corner of about 5 mRad on the outer edge, where the shower leakage of an incident electron is with energetic shower secondaries. The CONE shape allows the shower fully developed once the electron enters the calorimeter coverage. The shower leakage reaching the Fe-cone is recorded for the particle energies arriving and penetrating through, which are listed in Table **??** for 50 GeV and 125 GeV electrons. When the shower is well contained, the leakage is just a few dozens of less than 30 MeV particles. A shower on the edge creates up to 3k secondaries into the tracking volume mostly of less than 100 MeV. The 5 mm Fe layer can filter a large fraction of them, to less than 1k particles traversing through.

~~Scheme of a BGO luminometer with a diamond ring tracker.~~

1.7 Systematics on the integral luminosity

The main measure of luminosity at CepC is the count of Bhabha events $N_{\rm Bh}$ detected in coincidence in the two halves of the luminosity calorimeter LumiCal. The luminosity figure is then obtained from the equation of $\mathcal{L} = N_{acc}/\sigma^{vis}$. The cross section for the Bhabha process, σ_{vis}, should be integrated over the same phase space as used for the counting of Bhabha events. The limited precision with which the experimental acceptance region is defined gives rise to a number of systematic effects. Further, other processes misidentified as Bhabha and the limited accuracy of the theoretical calculation of σ_{vis} contribute to the overall systematic uncertainty.

A generator-level study was performed to assess the effects related to the precision of the Bhabha acceptance region on Bhabha counting. An underlying assumption of the study is that the LumiCal is centered on the outgoing beam axis. This assumption is essential for data-driven control of the radial offset of Lumical w.r.t. the IP, as well as

for Bhabha event counting based on the mirrored asymmetric polar-angle acceptance regions on the left and right side of the detector [4] (in further text, OPAL-style selection). OPAL-style counting cancels out biases due to left-right assymmetries of the experimental angular acceptance. It is further assumed that for the final state particles hitting the radial region between 50 mm and 75 mm, corresponding to the detector fiducial volume (FV), shower leakage has a negligible effect on he reconstruction of the polar angle and the energy.

Bhabha event samples are generated using the BHLUMI generator [1]. Center-of-mass (CM) energy of 240 GeVis assumed, roughly corresponding to the peak of the Higgs production cross section. The particles are generated in the range of polar angles including a ~ 7 mrad margin outside the FV to allow non-collinear final state radiation (FSR) to contribute to the events. After event generation, smearing is applied to the final particle vertices and momenta according to the nominal CepC parameters [5]. Additional smearing or bias is then applied according to one systematic effect at a time. Four momenta of close-by particles are summed up to account for cluster merging in LumiCal. The selection criteria to count an event consist of the OPAL-style angular selection and the requirement that the energy of both detected showers is above 50% of the nominal beam energy. The relative acceptance bias is determined as the relative difference between the Bhabha count $N_{\mathrm{Bh},i}$ obtained with the inclusion of the considered effect i and N_{Bh} obtained with the nominal set of parameters.

Table 1.3 lists the requirements on beam delivery, MDI and LumiCal installation, needed to limit individual systematic effects in the luminosity measurement to 1×10^{-3}, such as required for the Higgs program at CepC. Parameters influencing the integral luminosity precision are given as follows:

- ΔE_{CM}, uncertainty of the available CM energy affecting the Bhabha cross-section,
- $E_{e^+} - E_{e^-}$, asymmetry of the incident beam energies resulting in a net longitudinal boost of the event,
- $\frac{\delta\sigma_{E_{beam}}}{\sigma_{E_{beam}}}$, uncertainty of the beam energy spread,
- Δx_{IP} and Δz_{IP}, radial and axial offsets of the IP w.r.t. the LumiCal,
- Beam synchronization, resulting in axial offset of the IP w.r.t. the LumiCal,
- $\sigma_{x_{\mathrm{IP}}}$ and $\sigma_{z_{\mathrm{IP}}}$, radial and axial fluctuations of the scattering position,
- r_{in}, inner radius of the LumiCal acceptance region,
- $\sigma_{r_{\mathrm{shower}}}$, reconstruction precision of the radial shower coordinate,
- Δd_{IP}, uncertainty of the distance between the luminometer halves.

Most requirements are technically feasible with the present state of the art of accelerator and detector technology. The most important challenge identified is the precision of the inner acceptance radius r_{in} of LumiCal. In order to keep the luminosity precision of 1 permille, r_{in} must be known to within $10\,\mu\mathrm{m}$. The precision requirement of r_{in} scales linearly with the required luminosity precision, implying a correspondingly stricter requirement for the Z-pole run.

Table 1.3 Requirements on beam delivery, MDI and LumiCal installation, needed to limit **individual** systematic effects to 1×10^{-3}.

Parameter	unit	limit
ΔE_{CM}	MeV	120
$E_{e^+} - E_{e^-}$	MeV	240
$\frac{\delta\sigma_{E_{beam}}}{\sigma_{E_{beam}}}$		Effect cancelled
Δx_{IP}	mm	>1
Δz_{IP}	mm	10
Beam synchronisation	ps	7
$\sigma_{x_{\mathrm{IP}}}$	mm	1
$\sigma_{z_{\mathrm{IP}}}$	mm	10
r_{in}	mm	10
$\sigma_{r_{\mathrm{shower}}}$	mm	1
Δd_{IP}	μm	500

1.8 Summary

Instrumentation of the very forward region is very important for the realization of the CepC physics program. Several technology options are under consideration. Some of them have been successfully applied at LEP or are under study at other future projects. We argue that a tracker placed in front of the luminometer can improve polar angle measurement accuracy, facilitate LumiCal alignment and enable electron-photon separation. Luminometer must be centered on the outgoing beam axis to allow control of the systematic effects at the required level. Precision requirements on beam delivery, MDI and LumiCal installation have been addressed by simulation, and proven to be feasible with the present state-of-the-art of accelerator and detector technology.

References

[1] S. Jadach, W. Płaczek, E. Richter-Wąs, B. Ward, and Z. Wąs,
Upgrade of the Monte Carlo program BHLUMI for Bhabha scattering at low angles to version 4.04,
Computer Physics Communications **102** (1997) no. 1, 229 – 251. http://www.sciencedirect.com/science/article/pii/S0010465596001567.

[2] P. Janot and S. Jadach,
Improved Bhabha cross section at LEP and the number of light neutrino species,
Physics Letters B **803** (2020) 135319. https://www.sciencedirect.com/science/article/pii/S0370269320301234.

[3] R. Sadykov and V. Yermolchyk,
Polarized NLO EW e^+e^- cross section calculations with ReneSANCe-v1.0.0,
Computer Physics Communications **256** (2020) 107445.

https://www.sciencedirect.com/science/article/abs/pii/S0010465520302083.

[4] G. Abbiendi et al., Precision luminosity for Z^0 lineshape measurements with a silicon-tungsten calorimeter, The European Physical Journal C - Particles and Fields **14** (2000) 373–425. https://doi.org/10.1007/s100520000353.

[5] CepC parameter list, Available online. http://cepc.ihep.ac.cn/intro.html.